NUMERICAL SIMULATION OF BIRD-ENGINE BLADES STRIKE USING SPH METHODE

KADA ZEMANI* and HANA SLAMANI†

* Ecole Supérieure des Techniques de l'Aéronautique, Algiers, Algeria.

† Research Center in Industrial Technologies, BP 64, Cheraga, Algiers, Algeria.

kadazemani2@gmail.com – h.slamani@crti.dz

Abstract

Bird strikes are one of the most dangerous incidents occurring to aircraft engines and can inflict heavy casualties and economic losses, and multi-bird strikes are also frequently reported. In this paper, a numerical multi-bird-strike investigation, of engine fan blades subjected to bird-strike impact, was performed. The simulations were achieved using the finite element method (FEM). The numerical modeling of the bird strike investigation was conducted employing smooth particle hydrodynamics (SPH) with an EOS state equation. As most bird strikes transpire during take-off and landing, the bird was modeled with a set velocity of 70m/s and is impacted on the engine blades. The engine fan blades were modeled as a finite element method (FEM) and are rotating at 260 rad/s. Impact analyses have been presented using different impact scenarios and impact location distributions. The results are manifested as effective stresses, which show the structural damage and deformation of the engine blades struck by the birds. The small flocking bird strikes had different effects on the fan compared to the cases of medium flocking birds and large single bird. Further, the damage to the engine varies greatly with different impact locations and bird mass impacting blades. The use of a larger mass of birds and a higher impact location led to an increase in the threat to flight safety.

1. Introduction

A bird strike is a sudden and frequent accident that poses a serious threat to aviation flight safety. Structural bird-strike resistance should be evaluated during the design stages of aircraft components such as fan blades and airframe parts. Numerous studies on bird strikes have been carried out [1]. Previous studies focused on single bird strikes on engines, whereas in practice aircraft were often struck by flocks of birds. In 2009, both engines of United States (US) Airways Flight 1549 lost thrust after encountering a flock of birds and ditched on the Hudson River [2]. According to Federal Aviation Administration (FAA, Washington, DC, USA) statistics, there were 141,067 bird strikes between 1990 and 2020, with strikes by multiple birds 19,484 times, accounting for 13.8% of the total [3]. To confirm bird numbers and weights in future certification testing requirements, a relationship between bird flock density and a biometric factor has been described [3].

The earliest method of studying bird strikes was the experimental tests, which provided a direct method to assess the bird strike severity [4]. However, it is time-consuming and costly to design and carry out bird strike experiments [5]. The development of computer technology and the improvement of numerical simulation methods have provided a new approach for bird strike studies. Combined experimental and numerical approaches can provide feasible and cost-effective outcomes for bird strike studies [6]. In both experimental and simulation studies, bird modeling has always been a key question. To improve the accuracy of bird substitute models, the International Bird-strike Research Group (IBRG, Amsterdam, The Netherlands) studied the biometric data of different bird species and proposed a relationship between bird mass and the substitute model's geometric parameters [7]. There are currently four mainstream models used to replace real birds in experiments and simulations: namely the sphere, ellipsoid, straight-ended cylinder, and hemispherical-ended cylinder models.

Numerous aspects of the aircraft, such as the structural integrity, materials, and engine blades [8], must be made strong such that these impacts do not result in aircraft failure. Aircraft engines must resist the bird ingestion and still be able to last flight after the initial impact. As the bird strikes the aero-engine fan blades, the bird's momentum is then transferred to the blade during high-velocity impacts due to the blade's rotational oscillations, as discussed by Wilbeck [9]. Recently, the parametric study of bird strikes has been increasing. Bird impact to rigid plate scenarios are usually implemented to evaluate the efficiency of different bird model geometries [10]. To further understand the influence of the fan structure, the impact target model needs to be changed from a flat plate to a real engine.

It was observed that a few studies involving multi-bird and flocking bird strikes on fans. The multi-bird strike differs from that of a single bird in that the impact mass is larger and more blades are in contact. This research was conducted to investigate the numerical modeling of a flocking bird strike with the Smoothed Particle Hydrodynamics (SPH) method on rotating engine blades. The investigation assesses the damage output of the blades during this motion that causes severe damage to the engine blades. To study the hazards of flocking birds striking a fan, the SPH model was applied to simulate different birds and meet the requirements for multi-bird-strike simulations. Only a few blades were considered for numerical simulation, to obtain the blade stress distribution and impact deformation. The study in this paper contributes to a preliminary understanding of flocking bird impact effects and provides a reference for the development and modification of requirements for bird-strike airworthiness in aero engines.

2. NUMERICAL MODEL

1.1 Bird Geometry and Material Modeling

Several research had been conducted on numerical bird substitute models. Wilbeck performed many bird-strike tests and provided many test results [10]. Hedayati et al. [11] compared four traditional models, and the results showed that the hemispherical-ended cylinder was closer to the bird model in the experimental test. I. Smojver et al. [12]. and Chandra, C. et al. [13] both used hemispherical-ended cylinders to carry out bird-strike simulations and obtained acceptable results. In previous studies [14], the hemispherical-ended bird model has been proven to be accurate. Whereas traditional models were merely a simplification of the real bird body, in recent years three-dimensional (3D) scanning technology has been used to build a real-bird model, allowing the effect of body parts (head, tail, wings, etc.) on bird strikes to be studied [15]. However, this model can only be used for specific birds, cannot change their volume and mass, is difficult to modify, and is not well-suited to multi-bird strikes. Therefore, the hemispherical-ended substitute model was used in this simulation. The bird geometric model is shown in Figure 1. The length-to-diameter ratio is the key parameter in this model. Many studies have been performed on suitable geometric models, and a hemispherical-ended cylinder with a length-to-diameter ratio of 2 was proposed [11] (i.e., l/d=2), where l and d are the length and diameter of the hemispherical-ended model. To determine the l and d for each model, we introduce the equation for calculating hemispherical-ended volume:

$$V_h = \pi \left(\frac{d}{2}\right)^2 l + \frac{4}{3} \pi \left(\frac{d}{2}\right)^3 = \frac{\pi}{4} d^2 l + \frac{\pi}{6} d^3$$
 (1)

 V_h is the hemispherical-ended volume, combined with the mass calculation equation:

$$m_h = \rho V_h \tag{2}$$

 m_h is the bird mass, ρ is the bird density. The diameter of the bird substitute model can be calculated by:

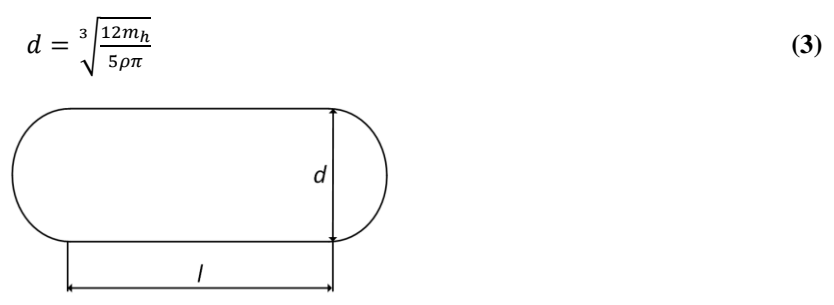


Figure 1: The hemispherical-ended cylinder geometric model

According to airworthiness standards [3], bird ingestion requirements have been defined for a large single bird and small and medium flocking birds. As the applied engine inlet throat area is $7 \, \mathrm{m}^2$, suitable bird parameters were selected for the simulation experiments, as shown in Table 1.

The Smoothed Particle Hydrodynamics (SPH) method is a Lagrangian meshless method used to model the motion of a continuum (fluids and solids). As in any Lagrangian method, the material history is easily tracked because particles are identified with a material point and as the material deforms the particles move with it. The SPH method is very good for modeling problems associated with impact characterized by large displacements, strong discontinuities, and

complex interface geometries [16]. The SPH method was used to discretize the bird model. The large bird model consisted of 36 000 SPH particles, with each particle weighing 0.076 g. The medium bird SPH particles totaled 18 000 and weighed 0.068 g each. The small flocking birds were discretized with 17 776 particles, each weighing 0.0047 g.

Table 1: Bird parameters

Categories	Bird Quantity	Bird Weight (Kg)	d (mm)	Density (kg/m ³)	R_{imp} (m)	
					0.5	
Large bird	01	2.75	130	950	1.0	
					1.5	
Medium bird	02	1.15	97	950	1.5	
Small bird	05	0.085	41	950	1.5	

For the bird properties, Wilbeck [10] showed that the stresses generated during a high-speed bird impact significantly exceed the tissue strength of the bird and that the bird behaves like a fluid with negligible viscosity. The inhomogeneity and nonuniformity due to other components such as feathers and bones can be neglected [17]. Based on this assumption that all parts bird body exhibit the same mechanical behavior, a single material model can effectively predict the impact behavior of the bird body under different conditions [18]. To simulate this material behavior of the bird body, a material model accompanied by an equation of states (EOS) is usually used. The null material model is often used to simulate fluids in high-velocity conditions. The strain of the fluid could be related to its stress by:

$$\sigma_{ij} = -P\delta_{ij} + 2\rho\gamma\dot{e}_{ij} \tag{4}$$

Where σ_{ij} is the viscous stress, P is the pressure on the fluid, δ_{ij} is the identity tensor, ρ is the fluid density, γ is the dynamic viscosity coefficient, and \dot{e}_{ij} is the rate of deformation tensor. The relative volumetric strain for erosion in tension and the relative volumetric strain for erosion in compression of the bird model are respectively 1 and 0.8. The EOS is linked to the material's physical state variables and is often applied in interpreting the properties of fluids and solids. For this, the Murnaghan EOS was chosen. The parameters used in this simulation B=128MPa and $\gamma=7.98$ were taken from McCarthy [19].

1.2 Engine blade Geometry and Material Modeling

For impact targets, which evolved from flat plates in the beginning to the current rotating blades, blades differ in terms of configuration and material. Single straight blades were first used [20], but this model did not reflect the bird-strike process well, as birds tended to contact with multiple blades. While straight blades were simple, the twist of the blades also influenced bird-strike results [21]. The fan materials were mainly rigid at the beginning, and the blades could not be deformed during impact, which was not in line with reality [22]. Based on the characteristics of the blade material, materials that could reflect the blade's elasto-plastic under dynamic loading were used in simulations. The Johnson-Cook material model, which can consider blade yield deformation and even fracture, is now widely applied [23, 24].

In the present simulation, only a few blades were considered to reduce computational time [25], as shown in Figure 2(a), together with the hub section. The target blades are modeled using the Johnson-Cook material model, while the hub is assumed to be rigid in comparison with the blade.

In order to remove mesh sensitivity and demonstrate convergence several simulations were performed with different blade mesh densities. The mesh chosen for the parametric studies presented in this paper comprises 175882 tetrahedron solid elements. The blade mesh and dimensions are shown in Fig. 2 (b). Corresponding radiuses are measured from the axis of rotation of the rotor. The external radius (R_{ext}) is measured to the tip of the blade, the internal (R_{int}) is measured to the root of the blade and the impact radius (R_{imp}) defines the initial position of the bird's center of mass.

Mao et al. [26] describe bird strike as an event characterized by: (i) High elastic and inelastic strains, (ii) High strain rates, and (iii) Short duration with very high intensity. In order to accurately model bird strikes and reproduce relevant physics, the Johnson-Cook visco-plasticity material model was selected to simulate the behavior of the blade. This material model takes into account plastic strain, strain rate, and temperature effects and therefore is appropriate for bird strike modeling [12, 27]. In the Johnson-Cook material model, the flow stress is expressed by [28]:

$$\sigma_{v} = (A + B\bar{\varepsilon}^{p^{n}})(1 + cln\dot{\varepsilon}^{*})(1 - T^{*m})$$
(5)

where A, B, n, c and m are the constants of the material (Table 2); $\bar{\varepsilon}^p$ is the effective plastic strain; $\dot{\varepsilon}^*$ is a unitless rate which can be obtained by dividing the quasi-static threshold rate by effective plastic strain rate; $T^* = (T \times T_m)/(T \times T_r)$ is the homologous temperature, T is the current temperature, T is the melt temperature of the material, and T is the room temperature. The strain at failure is defined as follows [28]:

$$\varepsilon^{f} = [D_{1} + D_{2}expD_{3}\sigma^{*}][1 + D_{4}ln\varepsilon^{*}][1 + D_{5}T^{*}]$$
(6)

where ε^f is the strain at fracture; D_1 , D_2 , D_3 , D_4 , D_5 are the failure parameters depending on the material; and σ^* is the stress triaxiality. Since the stress state, strain rate, and temperature are changing during the failure process, the failure of the material is determined by the following equation:

$$D = \sum \frac{\Delta \bar{\varepsilon}^p}{\varepsilon^f} \tag{7}$$

where D is the damage parameter and $\Delta \bar{\varepsilon}^p$ is incremental changes in the effective plastic strain. When the value of D reaches 1, the material can be considered as failed. The blades were made of titanium alloy Ti-6Al-4V; the material parameters are given in Table 2. As with the bird modeling, when using the Johnson-Cook material model, it is requisite to define an EOS for the material model. The Gruneisen EOS was adopted for this simulation (Table 3).

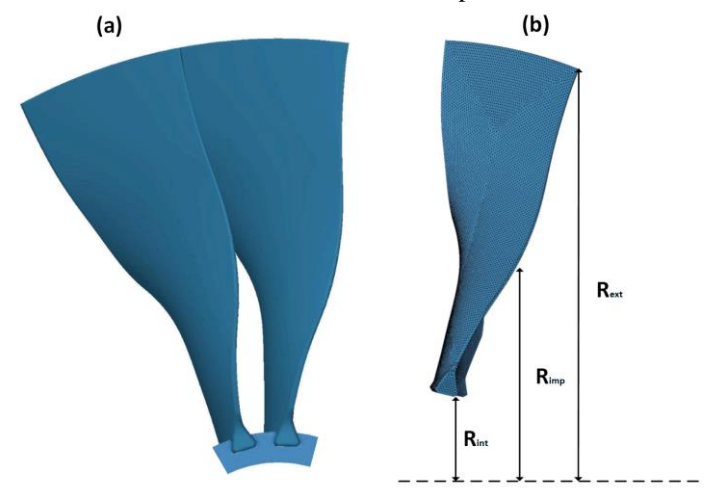


Figure 2: The finite element engine fan model used in simulation: (a) Parts of the numerical model (blades and part of the Hub), (b) Blade mesh and dimension measured from the leading edge.

Table 2: Johnson-Cook material parameters for Ti-6Al-4V

Parameter	Value			
Density	$\rho = 4420 \ kg/m^3$			
Shear modulus	G = 41.9 GPa			
Yield stress	A = 1098 MPa			
Strain hardening modulus	B = 1092 MPa			
Strain hardening exponent	n = 0.93			
Strain rate dependence	c = 0.014			
coefficient				
Softening exponent	m = 1.1			
Melting temperature	$T_M = 1878 K$			
Room temperature	$T_R = 293 K$			
Specific heat	$C_P = 612 J/Kg.K$			
	$D_1 = 0.112$			
	$D_2 = 0.123$			
Ecilium momentum	$D_3 = 0.48$			
Failure parameters	$D_4 = 0.014$			
	$D_5 = 3.87$			
•				

Table 3: Parameters used in Gruneisen EOS for Ti-6Al-4V

Parameter	C (m/s)	S_1	S_2	S_3	γ_0	а
Value	5130	1.028	O	0	1.23	0.17

1.3 Settings Simulation of Bird Striking on a Rotating Fan

In bird-Fan strike simulation, the bird impact involves interaction between one or more birds and one or more blades, hence using an appropriate contact algorithm is important in modeling the impact event. The contact between bird SPH particles and the fan FE elements was nodes-to-surface, which is one of the main approaches for contact treatment [25]. The bird-strike boundary conditions were the same, except for the different bird weights, quantities, and locations. Each bird's initial velocity was 70 m/s (280 km/h), while the fan was given an angular velocity of $\omega = 260$ rad/s (2500 tr/m). The bird's initial velocity was the initial relative speed of the bird and the engine, i.e., the ingestion speed.

The appropriate level of mesh refinement in finite element (FE) analysis is contingent upon the specific objectives of the study. When the objective is to accurately capture the shape of components during simulation, a minimum mesh density is required. In such cases, validating the mesh through a mesh sensitivity study is highly recommended. Mesh sensitivity is an inherent consideration in FE simulations, particularly when analyzing the impact behavior of materials. To assess whether the mesh is sufficiently refined, the analyst should incrementally increase the mesh density and rerun the simulation. Results which do not change significantly after refining the mesh would give confidence to the analyst that the original, coarser mesh is sufficient for the purpose of the simulation. On the other hand, significant discrepancies between the refined and original results suggest that the original mesh may be insufficiently refined.

Therefore, four primary simulations were carried out with different mesh densities in this study. Figures 3 and 4 gives the blades mesh density for each of the meshes and presents the internal energy of the system obtained for each analysis. All simulations were performed in a workstation with Intel(R) Core(TM) i7-6600U CPU @ 2.60 GHz 2.81 GHz and 16 GB RAM.

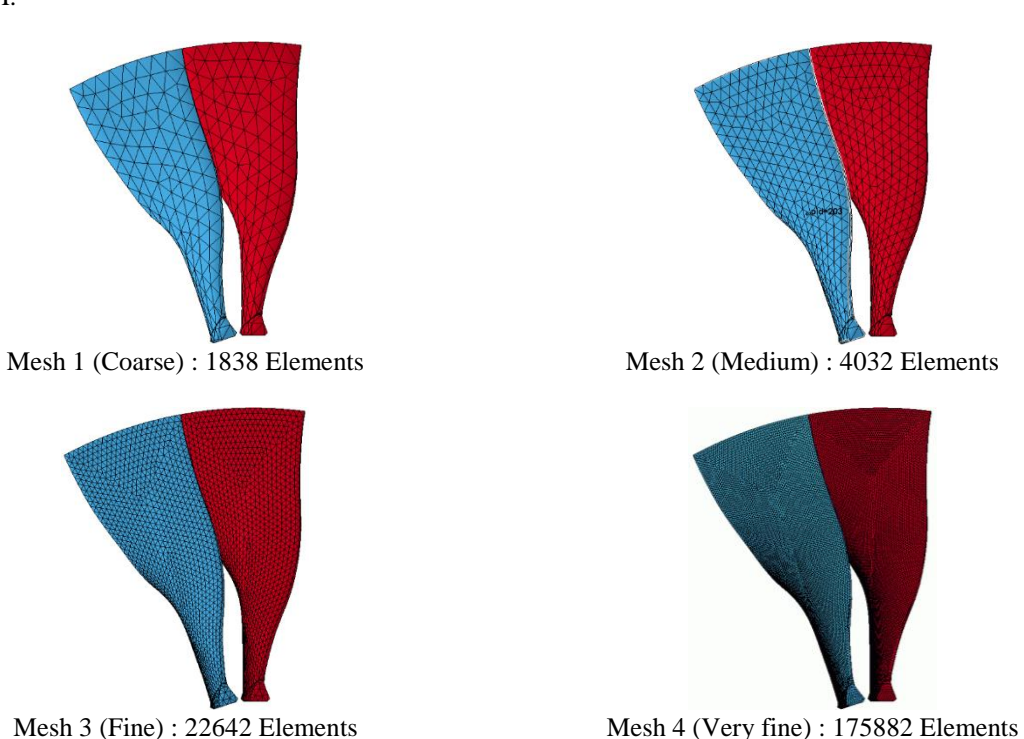


Figure 3: Meshing density types of the blades.

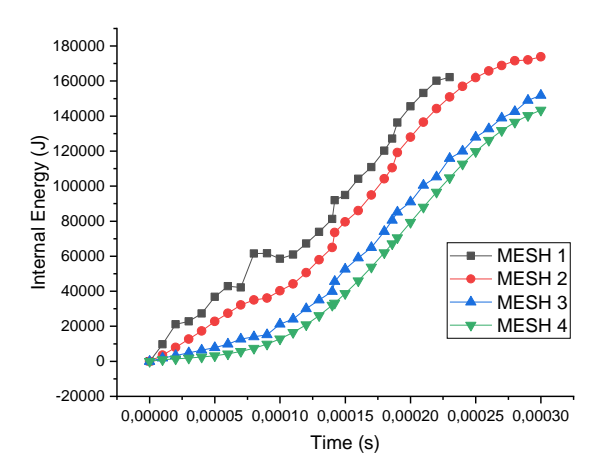


Figure 4: Variation of internal energy for four different meshes with respect to time.

The effect of mesh sensitivity on the variation of the internal energy as a function of time is shown in Figure 4. The figure shows that mesh 1 is far from representing a good level of internal energy due to unstable variation of internal energy values with time variation. However, when the mesh refinement increases, the difference in internal energy between 2 consecutive meshes decreases. The convergence of internal energy levels for mesh 3 and 4 indicates good energy conservation. Figure 4 demonstrates that, for a mesh composed of specimen elements number greater than 175882 significantly increasing computational expense. We will therefore use the most convergent mesh (i.e., mesh 4) in this case due to limitation of our workstation.

3. RESULTS AND DISCUSSION

In this paper, the impact of a large single bird and small and medium flocking bird strikes on the fan blades were investigated by numerical simulation analyses, focusing on the stress distribution on the blades, the deformation and damage on the fan, which determine how the engine is affected in this event. The damage to the fan caused by birds of different mass and different location of bird impact locations was also analyzed.

The large rotating radius of the fan blades made preloading the blades necessary. Several studies had investigated the influence of blade pre-stressing and found that it significantly affects blade deformation [20]. The pre-stress analysis of the fan can determine the stress distribution and deformation of the blade due to centrifugal force, which helps to obtain more accurate results from bird strike simulation. Fan rotational speed was 260 rad/s, which was generally the take-off speed of the engine. A dynamic relaxation was applied to obtain the Von Mises stress distribution. Results are shown in Figure 5. The maximum stress of the fan was about 13332 MPa, lower than the set yield strength. Therefore, the operation of the engine was normal before the bird strike occurred. The Von Mises stress was higher at the blade root. After the pre-stress analysis of the fan, the bird's impact on the rotating fan can be simulated.

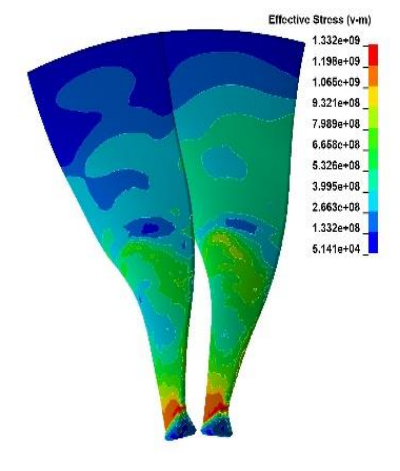


Figure 5: Initial effective V-M stress (Pa) in the system due to centrifugal force.

The bird-flock-strike setting required in the airworthiness manual [3] stated that the birds must be targeted to the first exposed locations and evenly distributed over the engine face area. To study the effect of different impact parameters on the bird strike, different case scenarios of the above-mentioned parameters were chosen for simulation. Combining the selected engine structure with the research objectives, five calculation cases were set up in this paper as shown in Figure 6 and Table 1. The numerical model presented in Figure 6 (c, d, e) will be used to study the effect of the bird flocks striking the engine blades. The models shown in Figure 6 (a, b, c) will be used to study the effect of impact location on the response of fun blades. The impact locations on the blade were chosen to be at 1/3 ($0 < R_{imp} \le 0.5m$), 2/3 ($0.5m < R_{imp} \le 1m$) and 3/3 ($1m < R_{imp} \le 1.5m$) of the engine radius. Note that the blade geometry, the mesh density, the boundary conditions, and the mechanical properties of the bird and blades in all simulations are kept the same as the input simulation. The only variables are the geometry, the particle number, and the location of the birds.

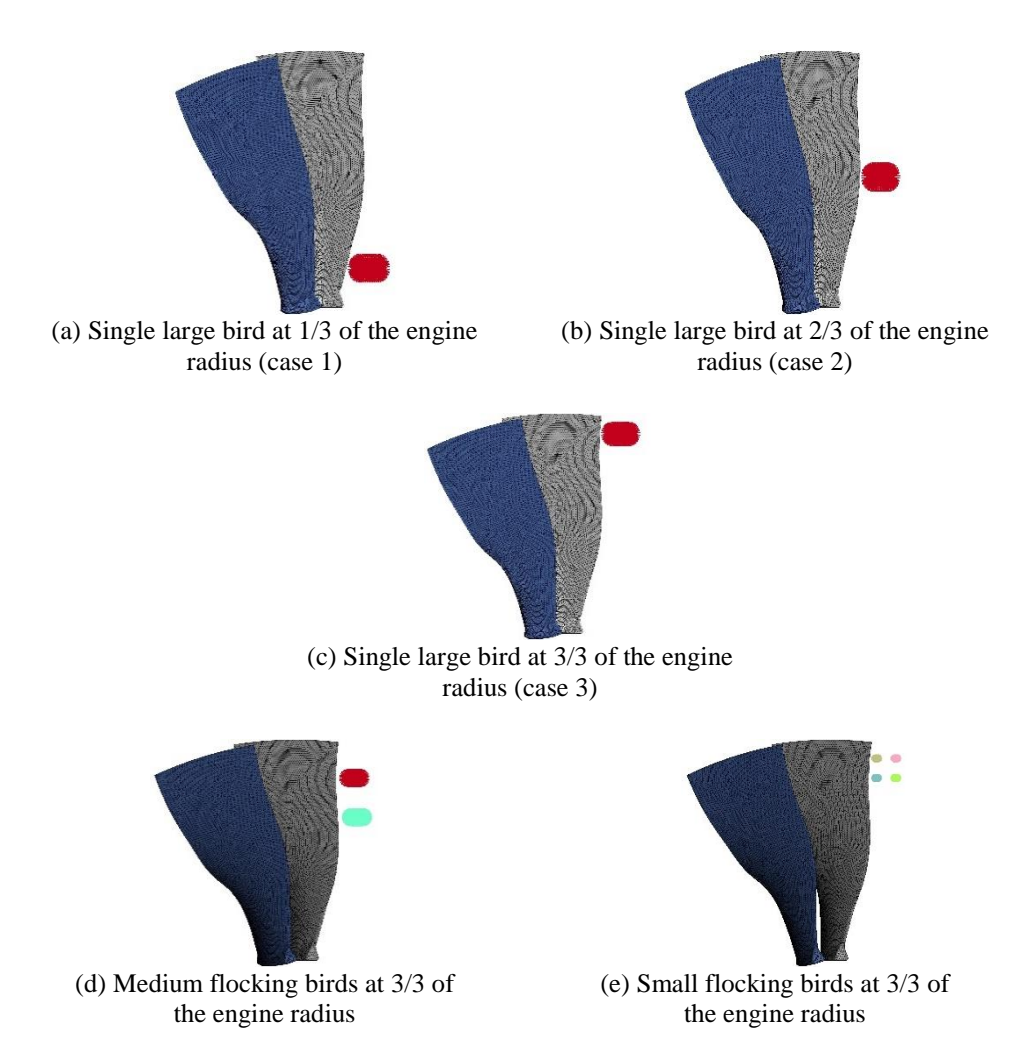


Figure 6: Different case studies considered for studying different parameters in the bird strike simulations.

The distribution of Von Mises stress under three different impact location distributions 1/3, 2/3, and 3/3 of the engine radius (see Figure 6 (a, b, and c)) with single large bird is shown in Figure 7. As shown in the figure, the higher stress areas were concentrated at the leading edge in direct contact with the bird body, and the root of the blades in all cases. The difference in the maximum of Von Mises stress was pronounced. In case 1 (striking on the 1/3 engine blades radius, Figure 7 (a)), the value for maximum stress in impact area was 1065 MPa, whereas the value in case 2 (striking on the 2/3 engine blades radius, Figure 7 (b)) was 1216 MPa. The maximum Von Mises stress developed in impacting blade area for case 3 (striking on the 3/3 engine blades radius, Figure 7 (c)) reached 1520 MPa. The stress maximums in cases 2 and 3 were both beyond the material yield stress (1098 MPa) in the impact area; blades would be permanently deformed in these cases, causing damage to the engine. This damage would be much less in the case 1. Overall, the maximum values of Von Mises stress occurred in case 3 (Large single bird striking on the blade tip), which represents the most dangerous scenario. Additionally, Figure 7 (c) illustrates the fan damage caused by the large bird in the tip of

the blade, these damages are characterized by material erosion in the leading edge in direct contact with the bird body, attended by tip bending of the blades, represent a threat to flight safety.

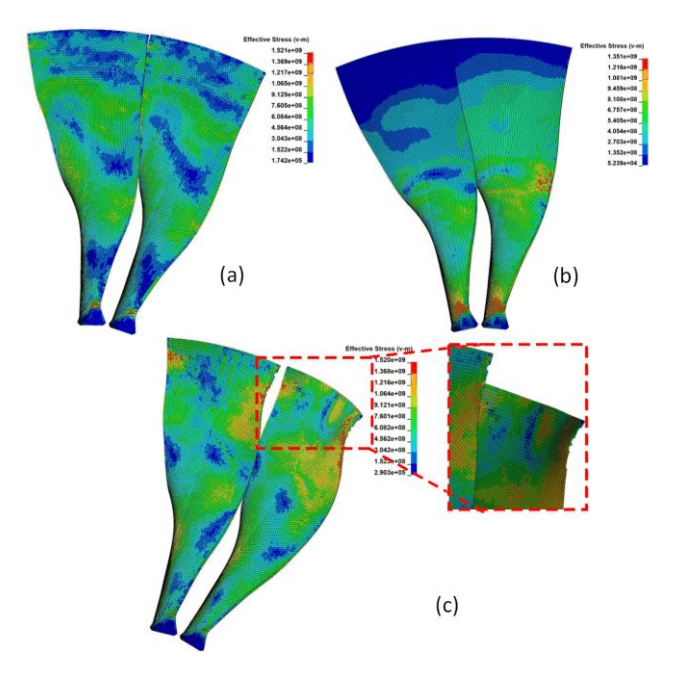


Figure 7: Distribution of Von Mises stress under three different impact location distributions in: (a) case 1, (b) case 2, (c) case 3

The distribution of Von Mises stress under three impact scenarios (small and medium flocking birds, and large single birds impacted the tip fan blades) is shown in Figure 8. The stresses generated by the single large bird and medium flocking birds were distributed over a larger area than in the scenario of the small flocking bird. It is worth noting that the maximum Von Mises stress also occurred close to the root of the blades in all scenarios.

In addition, the stress maximums of the small flocking birds (Figure 8 (a)), medium flocking birds (Figure 8 (b)) and the single large bird (Figure 8 (c)) impacting the fan were 1340, 1519, and 1520 MPa, respectively. The damage was less pronounced in small flocking birds scenario compared to single large and medium flocking striking scenarios, thus the small flocking birds impacting on the blades would increase the Von Mises stress on the fan but with less damage. In addition, in all scenarios, the Von Mises maximum stress was beyond the material yield stress; blades would be permanently deformed in these cases, causing damage damage in the direct contact area (deformation of the close neighborhood of the impacted area). However, comparing the medium birds with the small birds, the greater the mass, the greater the stress generated. Nevertheless, these results show the risk that can be reached after the blade impact, even in the case of small birds.

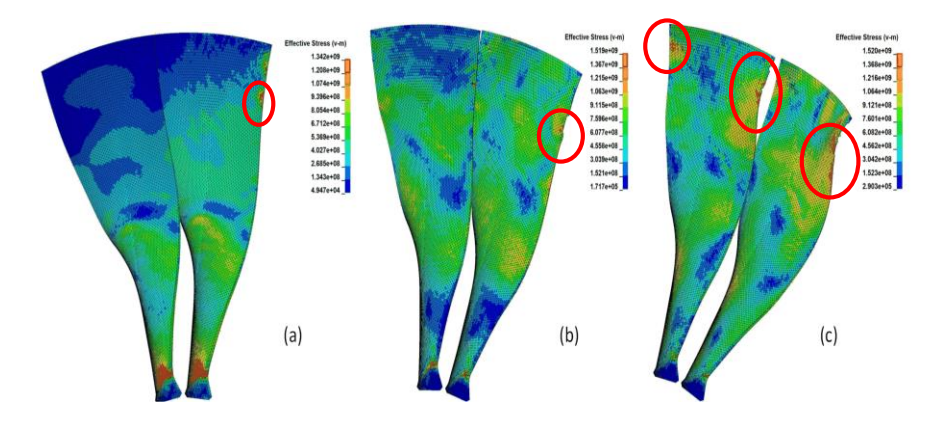


Figure 8: Von Mises stress distribution under three different impact scenarios: (a) Small flocking birds, (b) Medium flocking birds, (c) single large bird.

4. CONCLUSION

To investigate the effect of a bird's impact parameters on blade damage, an SPH bird model was used in this paper to simulate the process of bird impact. Tow parameters (impact location and flocking bird strikes scenarios) have been considered in the simulation. The distribution of impact locations affects the magnitude of the stresses on the blades. An increase in R_{imp} increases stress level. In other words, the impact on the blade tip is more dangerous compared to the impact on the blade root or the middle part, the risk of a bird strike becomes more severe in the impact in the tip region. The bird strike causes plastic deformation in the blade, leading to an increase in a threat to flight safety.

The total bird mass has a significant effect on the bird-strike process. The small flocking bird strike had little effect on the fan, whereas medium flocking birds and the single large bird will lead to an obvious variation of stresses, which may cause the stress concentrated area to undergo large deformation and even fracture due to exceeding the yield strength of the fan blades.

The damage to the engine varies greatly with different impact locations and birds mass impacting blades. Combined with the above results, the use of a larger mass of birds and a higher R_{imp} impact location in impact tests would allow for more severe test conditions to be obtained to verify the bird impact resistance of the engine blades.

Variations in airfoil structure can affect the bird-strike results and the conclusions may not apply to all engine types. These results could guide the design of test conditions and forthcoming studies, with an understanding of the effects of impact, the bird strike model can also be used to simulate other parameters such as initial bird velocity, and fan rotational speed using different geometries of birds.

References

- [1] S. J. C. Heimbs and Structures, "Computational methods for bird strike simulations: A review," vol. 89, no. 23-24, pp. 2093-2112, 2011.
- [2] E. Atkins, "Emergency landing automation aids: an evaluation inspired by US airways flight 1549," in AIAA Infotech@ Aerospace 2010, 2010, p. 3381.
- [3] F. A. J. F. A. Regulation, "part 33, Airworthiness Standards: Aircraft Engines," pp. 332-371, 2011.
- [4] J. Liu, Y. Li, and X. J. I. J. o. I. E. Gao, "Bird strike on a flat plate: Experiments and numerical simulations," vol. 70, pp. 21-37, 2014.
- [5] R. V. J. J. o. F. A. Kumar and Prevention, "Failure analysis of rotorcraft composite end plate structure under high-velocity bird impact," v, 2016.
- [6] E. Yuniarti and S. A. J. P. S. I. A. Y. Sitompul, "Initial Modelling of Bird Strike by Numerical Simulation in Varied L/D Ratio of Bird Geometry," vol. 4, pp. 443-452, 2018.
- [7] R. Budgey, "The development of a substitute artificial bird by the international birdstrike research group for use in aircraft component testing," in *Proceedings of the 25th Annual Meeting of the International Bird Strike Committee, IBSC25/WP-IE3. Amsterdam,* 2000, pp. 17-21.
- [8] N. A. Abdullah, M. Akbar, N. Wirawan, and J. L. J. C. S. Curiel-Sosa, "Structural integrity assessment on cracked composites interaction with aeroelastic constraint by means of XFEM,", 2019.
- [9] J. S. Wilbeck and J. L. Rand, "The development of a substitute bird model," 1981.
- [10] J. S. Wilbeck, Impact behavior of low strength projectiles. Texas A&M University, 1977.
- [11] R. Hedayati and S. J. I. J. o. C. Ziaei-Rad, "Effect of bird geometry and orientation on bird-target impact analysis using SPH method," vol. 17, no. 4, pp. 445-459, 2012.
- [12] I. Smojver and D. J. C. s. Ivančević, "Numerical simulation of bird strike damage prediction in airplane flap structure," vol. 92, no. 9, pp. 2016-2026, 2010.
- [13] C. Chandra, T. Wong, and J. Bayandor, "Crashworthiness assessment in aircraft ditching incidents," in 27th congress of the international council of the aeronautical sciences, September, 2010, pp. 19-24.
- [14] B. Wu, J. Lin, R. Hedayati, G. Zhang, J. Zhang, and L. J. A. S. Zhang, "Dynamic responses of the aero-engine rotor system to bird strike on fan blades at different rotational speeds," vol. 11, no. 19, p. 8883, 2021.
- [15] D. Zhang, Q. J. A. S. Fei, and Technology, "Effect of bird geometry and impact orientation in bird striking on a rotary jet-engine fan analysis using SPH method," vol. 54, pp. 320-329, 2016.
- [16] D. Chevrolet, S. Audic, and J. Bonini, "Bird impact analysis on a bladed disk," in *RTO AVT Symposium on "Reduction of Military Vehicle Acquisition Time and Cost through Advanced Modelling and Virtual Simulation"*, held in Paris, France, 2002, pp. 22-25.
- [17] M. Siemann, S. A. J. C. M. i. A. M. Ritt, and Engineering, "Novel particle distributions for SPH bird-strike simulations," vol. 343, pp. 746-766, 2019.

- [18] R. Hedayati and M. Sadighi, *Bird strike: an experimental, theoretical and numerical investigation*. Woodhead Publishing, 2015.
- [19] M. McCarthy *et al.*, "Modelling bird impacts on an aircraft wing–Part 2: Modelling the impact with an SPH bird model," vol. 10, no. 1, pp. 51-59, 2005.
- [20] M. Puneeth and D. J. M. T. P. JayaPrakash, "Influence of bird mass and impact height on the fan-blade of an aero-engine," vol. 44, pp. 1028-1038, 2021.
- [21] S. N. J. P. o. t. S. i. t. A. o. E. Husainie, Chicago, IL, USA, "Bird strike and novel design of fan blades," pp. 15-18, 2017.
- [22] F. Allaeys, G. Luyckx, W. Van Paepegem, and J. J. I. J. o. I. E. Degrieck, "Characterization of real and substitute birds through experimental and numerical analysis of momentum, average impact force and residual energy in bird strike on three rigid targets: A flat plate, a wedge and a splitter," vol. 99, pp. 1-13, 2017.
- [23] S.-S. Shahimi, N. A. Abdullah, M. Hrairi, M. I. M. J. J. o. A. Ahmad, Astronautics, and Aviation, "Numerical investigation on the damage of whirling engine blades subjected to bird strike impact," vol. 53, no. 2, pp. 193-199, 2021.
- [24] S. A. Ritt, A. F. Johnson, and H. Voggenreiter, "Analysis of Bird Strike under Blunt and Splitting Impact," 2017.
- [25] R. Vignjevic, M. Orłowski, T. De Vuyst, and J. C. J. I. J. o. I. E. Campbell, "A parametric study of bird strike on engine blades," vol. 60, pp. 44-57, 2013.
- [26] R. Mao, S. Meguid, T. J. I. J. o. M. Ng, and M. i. Design, "Transient three dimensional finite element analysis of a bird striking a fan blade," vol. 4, pp. 79-96, 2008.
- [27] S. Moakhar, H. Hentati, M. Barkallah, J. Louati, and M. J. P. o. t. I. o. M. E. Haddar, Part B: Journal of Engineering Manufacture, "Parametric study of aluminum bar shearing using Johnson-Cook material modeling," vol. 235, no. 9, pp. 1399-1411, 2021.
- [28] B. Wu *et al.*, "Flocking Bird Strikes on Engine Fan Blades and Their Effect on Rotor System: A Numerical Simulation," vol. 9, no. 2, p. 90, 2022.